Use of surgical augmented intelligence maps can reduce radiation and improve safety in the endovascular treatment of complex aortic aneurysms

Rohini J. Patel, MD, MPH,

Arielle M. Lee, MD,

John Hallsten, MD,

John S. Lane, MD,

Andrew R. Barleben, MD, MPH,

Mahmoud B. Malas, MD, MHS,

San Diego, CA

Division of Vascular and Endovascular Surgery, Department of Surgery, University of California San Diego.

Abstract

Objective: The introduction of endovascular procedures has revolutionized the management of complex aortic aneurysms. Although repair has traditionally required longer operative times and increased radiation exposure compared with simple endovascular aneurysm repair, the recent introduction of three-dimensional technology has become an invaluable operative adjunct. Surgical augmented intelligence (AI) is a rapidly evolving tool initiated at our institution in June 2019. In our study, we sought to determine whether this technology improved patient and operator safety.

Methods: A retrospective review of patients who had undergone endovascular repair of complex aortic aneurysms (pararenal, juxtarenal, or thoracoabdominal), type B dissection, or infrarenal (endoleak, coil placement, or renal angiography with or without intervention) at a tertiary care center from August 2015 to November 2021 was performed. Patients were stratified according

to the findings from intelligent maps, which are patient-specific AI tools used in the operating room in conjunction with real-time fluoroscopic images. The primary outcomes included operative time, radiation exposure, fluoroscopy time, and contrast use. The secondary outcomes included 30-day postoperative complications and long-term follow-up. Linear regression models were used to evaluate the association between AI use and the main outcomes.

Results: During the 6-year period, 116 patients were included in the present study, with no significant differences in the baseline characteristics. Of the 116 patients, 76 (65.5%) had undergone procedures using AI and 40 (34.5%) had undergone procedures without AI software. The intraoperative outcomes revealed a significant decrease in radiation exposure (AI group, 1955 mGy; vs non-AI group, 3755 mGy; $P = .004$), a significant decrease in the fluoroscopy time (AI group, 55.6 minutes; vs non-AI group, 86.9 minutes; $P = .007$), a decrease in the operative time (AI group, 255 minutes; vs non-AI group, 284 minutes; $P = .294$), and a significant decrease in contrast use (AI group, 123 mL; vs non-AI group, 199 mL; $P < .0001$). No differences were found in the 30-day and long-term outcomes.

Conclusions: The results from the present study have demonstrated that the use of AI technology combined with intraoperative imaging can significantly facilitate complex endovascular aneurysm repair by decreasing the operative time, radiation exposure, fluoroscopy time, and contrast use. Overall, evolving technology such as AI has improved radiation safety for both the patient and the entire operating room team. (J Vasc Surg 2023;77:982–90.)

Keywords

Endovascular aortic aneurysm repair (EVAR) had transformed the repair of abdominal aortic aneurysms (AAAs) and the field of vascular surgery to a minimally invasive practice with many benefits reported from landmark clinic trials and real-world studies, including lower 30-day mortality, a lower incidence of complications, and a shorter hospital stay.[1–5] As one of the great technological advancements in the surgical field, the added risk of radiation exposure to the operating room team and patient has not always been apparent. Long-term exposure to radiation has been known to cause malignancies and cardiovascular disease, as was seen in a cohort of Japanese atomic bomb survivors.[6] As EVAR and complex aortic repairs, such as physician-modified endografts with fenestrations and branches (f/bEVAR), have become more common, the need to address radiation exposure and develop techniques to help mitigate the radiation dose per case is increased.

Several studies have documented the relationship between radiation exposure and vascular surgery. In 2015, a review of ionizing radiation during EVAR found that patient radiation exposure had greatly increased owing to surveillance computed tomography (CT) scans and that physician exposure is linked to the number of endovascular repairs performed annually, although few radiation-related injuries have been reported.[7] Similarly, a systematic review of 24 studies found that complex aortic cases resulted in a greater radiation burden and that education regarding radiation safety was not always a prominent feature of training.[8] A retrospective review of infrarenal EVAR found that the total number of anatomic risk factors,

such as aneurysm size, neck diameter, angulation, and body mass index (BMI), were the most important factors related to increased radiation exposure.[9,10]

Chronic low-dose radiation exposure has been studied infrequently. However, in the United Kingdom, operators who had not worn leg shields during f/bEVAR were found to have a higher amount of radiation-induced DNA damage.[11] The advent of hybrid operating rooms has introduced a new learning curve for endovascular repair but with the added benefit of higher quality images, better ergonomics, and greater ease. A retrospective review comparing hybrid operating rooms and conventional C-arm use did not find any differences in the radiation parameters, suggesting that surgeon experience is the main factor.[12]

A paucity of literature and evidence of the factors necessary to decrease radiation exposure during EVAR or f/bEVAR beyond the standard radiation safety practices are available. Given the increasing prevalence of complex aortic repair and, therefore, greater radiation exposure to both the operating room team and the patient, we investigated a technique to mitigate radiation exposure.[13,14] We studied a surgical augmented intelligence (AI) tool that was incorporated into the operating room to aid in three-dimensional (3D) visualization during complex aortic repair.

This specific AI tool has been used in >3000 cases worldwide. It is a cloud-based platform to allow for ease of integration into the vascular hybrid operating room. A preoperative map is created from the patient's CT scan, and marker rings are placed to identify the visceral orifices. The map is then superimposed with real-time fluoroscopic images during surgery. Together, this has allowed for easier identification, cannulation, and, ultimately, stent placement of visceral vessels. A previous single-institution study found that this tool can decrease radiation exposure and contrast during fEVAR.[15]

METHODS

Study population.

We performed a retrospective study of all patients who had undergone complex aortic aneurysm (pararenal, juxtarenal, or thoracoabdominal), type B dissection, or infrarenal (endoleak, coil placement, or renal angiography with or without intervention) repair at a single institution (University of California, San Diego) from August 2015 to November 2021. The institutional review board approved the present study and waived the requirement for individual patient consent owing to the de-identified nature of the present study. The demographic, clinical, and intraoperative data and shortand long-term outcomes were recorded for each patient. The inclusion criterion was complex aneurysm repair during the study period. The patients were stratified by the use of AI maps, which are patient-specific AI tools used in the operating room in conjunction with real-time fluoroscopic images. The patients were not randomized to either group. Use of the AI tool was instituted in June 2019 at our hospital and was used almost exclusively since then. For the cases after 2019 for which the software was not used, these had been performed during the transition period when we were learning how the tool could be implemented for nonfenestrated and nonbranched cases. The exclusion criteria were patients deemed fit for open repair by the

attending vascular surgeon and patients aged <18 years because the software requires the patient to have mature vertebral anatomy.

Measurements and outcomes.

A secure database was created using the electronic health records for all patients who had undergone complex aortic repair at our institution from August 2015 to November 2021. For each patient, the demographic, clinical, operative, and postoperative data were obtained. The demographic variables included age, sex, race, and medical comorbidities. The clinical variables included aortic aneurysm size, aneurysm type, symptomatic status, and procedure type (f/bEVAR, thoracic EVAR, EVAR). The primary outcomes included the operative time, radiation exposure, fluoroscopy time, and contrast use. The operative time was measured from the incision to closing, with the complete time measured in minutes. Radiation exposure was measured in milligrays to represent the air kerma, and the fluoroscopy time was measured in minutes by the hybrid operating room radiography machine. The contrast volume was measured in milliliters during operative administration. The secondary outcomes included 30-day postoperative mortality and complications such as paraplegia, respiratory failure, stroke, bowel ischemia, and renal failure. The long-term follow-up data included the aneurysm size at the most recent follow-up, the presence of an endoleak, reintervention, aneurysm rupture after repair, aneurysm-related mortality, and allcause mortality.

Technology.

All surgeons at our institution were trained in the use of this specific AI tool in the operating room. The tool is a cloud-based integrated solution (Cydar EV Maps, Cambridge, UK) that generates a patient-specific 3D map of the relevant arterial anatomy based on bony landmarks and updates in real time to optimize procedure planning and intraoperative navigation and allows for an assessment of the outcomes. The 3D virtual map can be used 30 minutes between the CT scan upload and surgery to assist in emergency cases. The patients in the AI group had undergone preoperative mapping. First, a preoperative CT scan of the chest, abdomen, and pelvis with intravenous contrast was obtained; however, this step can also be performed using nonecontrast-enhanced scans. The preoperative CT scan ideally should have a slice thickness of 1.0 mm, and each vertebra, including the spinous processes, must be included. Second, the preoperative CT scan was uploaded to a secure online vault, which identifies the patient by their name, birthdate, and a unique identifier. Third, a dynamic, patient-specific 3D map was created showing virtual blood vessels, guidewires, measurements, and markers. The measurements are patient specific at various points in the aorta, iliac vessels, and branch vessels that are determined and adjusted by the surgeon. The markers can be used to identify the origin of vessels such as the mesenteric and arch vessels in the preoperative map.

In the operating room, the preoperative map was loaded and image tracking initiated. Once fluoroscopy was initiated during the procedure and the lumbar vertebrae were in view, fluoroscopy was used to link the preoperative map to the current patient position and provide the overlay. Each time the view changes or wires alter the anatomy, the image tracking software will automatically readjust. Additionally, the technology will allow the surgeon to

micro-adjust the location of the vessel markers to the actual angiography imaging findings when the intraoperative anatomy has been deformed relative to the preoperative anatomy owing to changes in patient posture or the insertion of devices. Adjusting one vessel will result in the correction of all other visceral vessels by moving all markers in parallel and, thus, provides a real-time accurate map at all times. The ability to manually adjust the map in the operating room to account for deformational changes is one of the unique advantages of the Cydar AI tool compared with other developing systems[16] (Fig).

Overall, the AI tool creates a combined 3D reconstruction of the patient's aorta and visceral vessel origins through a combination of a patient-specific preoperative CT scan and live intraoperative fluoroscopic images. Traditionally, endovascular suites had to have been matched with company-specific AI software packages. However, Cydar is unique in that it can be paired with any currently available fixed endovascular suite hybrid operating room system or a portable unit such as a C-arm. During the entire study period, all cases were performed using the same endovascular suite.

Statistical analysis.

Continuous variables were assessed using the Student t test and Wilcoxon rank sum test and categorical variables using the χ^2 test of independence. Overall, <5% of our collected variables had had missing or incomplete data.

Our cohort was divided into two groups according to AI usage during complex aortic repair. Multiple linear regression was used to compare the outcomes of interest. The final models were created using a stepwise backward selection with $P < .01$ on univariate analysis and including clinically relevant variables. Model fit was assessed by R^2. A two-tailed alpha value of <0.05 was considered statistically significant. All data analyses used R studio, version R-4.1.0 (Boston, MA).

RESULTS

Study population.

Our cohort included all consecutive patients who had undergone complex aortic aneurysm repair at a single institution between August 2015 and November 2021, for a final cohort of 116 patients. Of these patients, 76 (65.5%) had undergone surgery with AI mapping (WAI) and 40 (34.5%) without AI mapping (WOAI). The mean age of the entire cohort was 73.1 ± 11.2 years. Complex repair was further divided into f/bEVAR, complex EVAR for type B dissection requiring EVAR or visceral vessel aneurysm or stenosis requiring EVAR, endoleak repair from previous EVAR, and thoracic EVAR (Supplementary Fig 1, online only).

Baseline characteristics.

In general, the two groups were similar at baseline. The WOAI group was older than the WAI group (75.5 ± 9.0 years vs 71.9 ± 12.0 years), with a greater proportion of women (22.5% vs 14.5%), chronic kidney disease (32.5% vs 26.5%), hyperlipidemia (50% vs 43.4%), a history of open AAA repair (5% vs 3.9%), and a history of EVAR

(37.5% vs 34.2%). The high proportion of patients with previous EVAR was because our institution is the only high-volume tertiary care center in the area. We receive many patients from outside hospitals who had undergone EVAR several years prior and had developed endoleaks requiring f/bEVAR that could not be performed at their current health center. The WAI group had had a greater history of cardiac disease at baseline, including atrial fibrillation (19.7% vs 17.5%) and congestive heart failure (17.1% vs 10.0%). Although these differences were clinically relevant, none were statistically significant. The only statistically significant difference was in the family history of AAAs (WOAI group, 10%; vs WAI group, 1.3%; *P* = .029; Table I).

Aneurysm characteristics.

No significant differences were found in aneurysm size, symptomatic status, or rupture status between the two groups (Table II). On average, 2.6 visceral vessels had been treated in the WAI group and 2.3 in the WOAI group (*P* = .479). Additionally, when the aneurysms were stratified by type or treatment indication (pararenal, juxtarenal, thoracoabdominal, type B dissection, thoracic, infrarenal [including endoleak or coil], or other [including visceral aneurysms or stenosis]), no significant differences were found between the two groups.

PRIMARY OUTCOMES

The univariate analysis results revealed significantly different outcomes for radiation exposure, fluoroscopy time, and contrast use (Table III). We found that radiation exposure for the WAI group was almost one half that for the WOAI group (1955 mGy vs 3755 mGy; *P* = .004). Furthermore, the fluoroscopy time was 30 minutes less for the WAI group (55.6 minutes vs 86.9 minutes; *P* = .008). Contrast use was also less in the WAI group (122 mL vs 199 mL; *P* < .0001). Although not statistically significant, a decrease was also found in the operative time for the WAI group (255 minutes vs 284 minutes; *P* = .294). Additionally, we created a ratio between the radiation dose and BMI and found that even after accounting for the BMI, a significant reduction remained in the radiation exposure for the WAI group (65.2 vs 139.7; *P* = .001). Finally, no significant differences were found in the estimated blood loss, units of packed red blood cells transfused, or amount of intravenous fluids administered. Over time, less radiation exposure had occurred, with an emphasis on when the use of the AI tool had been initiated (Supplementary Fig 2, online only).

Regression model.

The results from the adjusted linear regression models for the primary outcomes are presented in Table IV. After adjusting for age, sex, race, BMI, coronary artery disease, smoking status, history of EVAR, aneurysm size before repair, and aneurysm type, we found a significant decrease in contrast use, radiation exposure, and fluoroscopy time with AI use. With the AI tool, we found a decrease of 77 mL in the contrast used (*P* < .0001), a decrease of 2002 mGy in radiation exposure (*P* < .0001), and a decrease of 26 minutes in the fluoroscopy time (*P* = .007). Although a decrease in operative time had occurred, the difference was not significant. Overall, the multivariate model indicated that contrast use, radiation exposure, and fluoroscopy time were decreased with the use of fusion imaging.

Thirty-day postoperative outcomes.

We found no differences in the incidence of access-site complications, including hematoma, distal embolus, and pseudoaneurysms, and no differences in the length of stay. Additionally, no differences were found in the incidence of major complications after complex endovascular aortic repair, including stroke, bowel ischemia, lower extremity ischemia, renal failure, new-onset dialysis, and death in the perioperative period (Table V).

Long-term outcomes.

Overall, no differences were found in presence of the endoleak on repeat imaging, reintervention, aneurysm rupture after repair, changes in aneurysm size from preoperatively to the most recent follow-up, aneurysm-related mortality, or all-cause mortality (Supplementary Table, online only). Most of the endoleaks at follow-up were attributed to type II endoleaks (WOAI group, 45.5%; vs WAI group, 69.6%), with only one patient in each group with an endoleak attributable to an aortic side branch or side brancheside branch attachment. Additionally, none of our patients had experienced aneurysm rupture after repair or aneurysm-related mortality.

DISCUSSION

The introduction of minimally invasive endovascular repair has revolutionized the field of vascular surgery. However, minimally invasive endovascular repair has increased the risk of radiation exposure to the operating team and the patient and the risk of contrast-induced kidney injury to the patient.[17–19] A study by El-Sayed et al[11] was one of the first studies to find acute DNA damage in operators after branched and fenestrated aortic repair. We performed a retrospective review of prospectively collected data to study the effects of AI software incorporated into the operating room on the known risks of endovascular surgery. Most initial studies of image fusion in the operating room found a decrease in contrast use, similar to our study; however, in contrast to our study, they did not find a decrease in radiation levels.[20–23] AI technology, specifically the Cydar EV mapping used at our institution, is an improvement over first-generation 3D mapping because of two major advances: real-time adjustment using cloud-based technology and deformational adjustment due to stiff wires and devices. We believe that our significant reduction in radiation exposure had likely resulted from both the easier identification of the target vessel ostium and manual adjustment of vessel deformation as the wires and devices were inserted. Additionally, the AI tool allows operators to perform less digital subtraction angiography because the visceral orifices have already been identified.

Our study found a significant decrease in both radiation exposure and contrast use in the WAI group compared with the WOAI group, similar to the findings from small-volume, single-center reviews from Europe and the United States.[24–27] A prospective trial comparing simple infrarenal EVAR with 44 fusion AI patients and 21 controls found no significant difference in operating time or fluoroscopy time, with, however, a lower air kerma product in the fusion group (82 mGy vs 142 mGy in the control group) and overall fewer digital subtraction angiography runs in the fusion group.[24] A similar study of complex EVAR compared with a previously reported EVAR cohort found that the addition of fusion imaging

lowered radiation exposure.[25] Finally, a study of 30 cases of f/bEVAR using fusion imaging compared with 30 controls found that fusion imaging was beneficial in terms of procedure time and contrast volume administered but not the fluoroscopy time.[28]

A comprehensive literature review in Europe led to reporting standards and recommendations that all trainees undergo specific radiation safety training to apply the ALARA (as low as reasonably achievable) principle because of the amount of radiation exposure they would encounter in practice.[29] Previous studies have demonstrated the use of fusion imaging to assist intraoperatively with the anatomic distortion that occurs between the preoperative CT scan and the insertion of rigid wires that shift the visceral vessel ostium.[30] A study in Canada found that a combination of educational incentives, a slower frame rate, a lower radiation dose per pulse, and 3D mapping integration decreased the mean dose area product during interventional and electrophysiology procedures.[31] The current strategies to mitigate the radiation levels have had mixed results in the operating room. The use of dosimetry badges has not been found to change surgical practice when real-time data on high radiation doses are conveyed.[32]

A study of 100 patients with either thoracic aneurysm repair or abdominal aneurysm repair found that an increase of 10 minutes of treatment caused an increase in 80 Gy cm^2 in the dose area product, which is a surrogate measure for the total amount of x-ray energy delivered to the patient.[33] This finding was similar to our study, where we found that our WOAI cases had required, on average, a 30-minute longer fluoroscopy time, with almost double the radiation exposure. A meta-analysis in 2021 of 11 studies totaling 1500 patients found that complex EVAR repair with image fusion had required significantly less contrast volume, fluoroscopy time, and procedure time compared with the cases without image fusion.[34] This was similar to the findings from our analysis, except that we did not find a significant difference in the operative time between the WAI and WOAI groups. One explanation for this was that, overall, the complexity of our cases had increased over time. A similar meta-analysis of 900 patients across seven studies found a significant decrease only in the contrast volume for complex aortic repairs with the addition of 3D fusion imaging.[35]

Overall, use of the AI tool allowed vascular surgeons to incorporate a patient's preoperative CT scan with live intraoperative fluoroscopic images. This allows for easier identification of small visceral orifices, which, traditionally, have been more difficult to cannulate and require large amounts of radiation for proper visualization. The use of Cydar EV mapping differs from that of other currently available technology in that it is cloud based, able to interact with any hybrid operating room system or portable system, and, finally, that real-time adjustments of the map can be made in the operating room if deformational changes from wires or devices has occurred. At our institution, this tool was easy to incorporate for our four surgeons and has been the most beneficial with the f/bEVAR cases. As previously stated, we believe this technology can reduce radiation exposure and increase patient and operator safety because it allows for easier cannulation of the visceral orifices with less radiation needed for visualization.

Study limitations.

Our study had several limitations. First, the retrospective nature of the study did not allow for an accurate assessment of causation. Although our multivariate models attempted to control for significant confounders, a prospective study or randomized trial should be considered. Second, we performed the present study with a relatively small sample size and only at a single institution with vascular surgeons specifically trained and adept at using the AI software. Further studies should focus on larger sample sizes with more patient and surgeon variety. Third, future studies could focus on the operative time defined by the use of AI from wire insertion to the final angiogram to eliminate vessel access and closure times. Fourth, because the patients were prospectively added to the database with the start of AI in 2019, one could argue that surgeon experience had increased and the learning curve had decreased and could have contributed to our outcomes. However, we believe that by 2019 when AI usage was initiated, each surgeon at our institution had already had high-volume experience in complex aortic work. Finally, our study had a temporal bias. During the course of our study, most of the WAI procedures had been completed later in our operative experience. These cases were subjectively more complex and, as an institution, we were performing more difficult cases in part because we were using fusion imaging assistance.

Overall, during the course of our study, radiation awareness and safety had likely increased, in addition to the aforementioned technique changes that helped contribute to the decrease in radiation levels. In terms of the AI software, the Cydar EV maps has one inherent limitation. The link between the patient's preoperative map and fluoroscopic images relies on vertebral body identification. In the case of severe osteoporosis or the presence of spinal hardware, this could represent a potential limitation. However, to date, such cases have represented <1% of cases performed.

CONCLUSIONS

As complex endovascular procedures become more common and radiation exposure increases for both patients and operating room teams, the need for strategies to mitigate the risks associated with radiation exposure has increased in importance. Our study found that the use of cloud-based integrated augmented intelligence software in conjunction with real time fluoroscopic images in the operating room can reduce contrast use, fluoroscopy time, and radiation exposure compared with similar cases that did not use AI technology. We believe that this tool can decrease radiation exposure for the entire operative team and improve radiation safety for vascular surgeons. Further prospective or randomized clinical trials are needed to confirm our findings.

Supplementary Material

Refer to Web version on PubMed Central for supplementary material.

Acknowledgments

REFERENCES

1. Greenhalgh RM, Brown LC, Kwong GP, Powell JT, Thompson SG; EVAR Trial Participants. Comparison of endovascular aneurysm repair with open repair in patients with abdominal aortic aneurysm (EVAR trial 1), 30-day operative mortality results: randomised controlled trial. Lancet 2004;364:843–8. [PubMed: 15351191]

2. Patel R, Sweeting MJ, Powell JT, Greenhalgh RM; EVAR Trial Investigators. Endovascular versus open repair of abdominal aortic aneurysm in 15-years' follow-up of the UK endovascular aneurysm repair trial 1 (EVAR trial 1): a randomised controlled trial. Lancet 2016;388:2366–74. [PubMed: 27743617]

3. Prinssen M, Verhoeven EL, Buth J, Cuypers PW, van Sambeek MR, Balm R, et al. ; Dutch Randomized Endovascular Aneurysm Management (DREAM) Trial Group. A randomized trial comparing conventional and endovascular repair of abdominal aortic aneurysms. N Engl J Med 2004;351:1607–18. [PubMed: 15483279]

4. Malas M, Freischlag J. Interpretation of the results of OVER in the context of EVAR, DREAM and the EUROSTAR registry. Semin Vasc Surg 2010;23:165–9. [PubMed: 20826293]

5. Malas M, Arhuidese I, Qazi U, Black J, Perler B, Freischlag JA. Peri-operative mortality following repair of abdominal aortic aneurysms: application of a randomized clinical trial to real-world practice using a validated nationwide data set. JAMA Surg 2014;149:1260–5. [PubMed: 25337871]

6. Kamiya K, Ozasa K, Akiba S, Niwa O, Kodama K, Takamura N, et al. Long-term effects of radiation exposure on health. Lancet 2015;386: 469–78. [PubMed: 26251392]

7. Dindyal S, Rahman S, Kyriakides C. Review of the use of ionizing radiation in endovascular aneurysm repair. Angiology 2015;66:607–12. [PubMed: 25225195]

8. Monastiriotis S, Comito M, Labropoulos N. Radiation exposure in endovascular repair of abdominal and thoracic aortic aneurysms. J Vasc Surg 2015;62:753–61. [PubMed: 26169014]

9. Machado R, Ferreira VM, Loureiro L, Gonçalves J, Oliveira P, Almeida R. Radiation exposure in endovascular infra-renal aortic aneurysm repair and factors that influence it. Braz J Cardiovasc Surg 2016;31:415–21. [PubMed: 28076617]

10. Kakkos SK, Efthymiou FO, Metaxas VI, Dimitroukas CP, Panayiotakis GS. Factors affecting radiation exposure in endovascular repair of abdominal aortic aneurysms: a pilot study. Int Angiol 2021;40:125–30. [PubMed: 33315209]

11. El-Sayed T, Patel AS, Cho JS, Kelly JA, Ludwinski FE, Saha P, et al. ; Guy's and St Thomas' Cardiovascular Research Collaborative. Radiation-induced DNA damage in operators performing endovascular aortic repair. Circulation 2017;136:2406–16. [PubMed: 29054934]

12. Wermelink B, Willigendael EM, Smit C, Beuk RJ, Brusse-Keizer M, Meerwaldt R, et al. Radiation exposure in an endovascular aortic aneurysm repair program after introduction of a hybrid operating theater. J Vasc Surg 2019;70:1927–34.e2. [PubMed: 31327609]

13. Rolls AE, Maurel B, Davis M, Constantinou J, Hamilton G, Mastracci TM. A comparison of accuracy of image- versus hardwarebased tracking technologies in 3D fusion in aortic endografting. Eur J Vasc Endovasc Surg 2016;52:323–31. [PubMed: 27389943]

14. Varnavas A, Carrell T, Penney G. Fully automated 2D-3D registration and verification. Med Image Anal 2015;26:108–19. [PubMed: 26387052]

15. Bailey CJ, Edwards JB, Giarelli M, Zwiebel B, Grundy L, Shames M. Cloud-based fusion imaging improves operative metrics during fenestrated endovascular aneurysm repair. J Vasc Surg 2023;77:366–73. [PubMed: 36181994]

16. Dupont C, Kaladji A, Rochette M, Saudreau B, Lucas A, Haigron P. Numerical simulation of fenestrated graft deployment: anticipation of stent graft and vascular structure adequacy. Int J Numer Method Biomed Eng 2021;37:e03409. [PubMed: 33098246]

17. Weerakkody RA, Walsh SR, Cousins C, Goldstone KE, Tang TY, Gaunt ME. Radiation exposure during endovascular aneurysm repair. Br J Surg 2008;95:699–702. [PubMed: 18446782]

18. Ho P, Cheng SW, Wu PM, Ting AC, Poon JT, Cheng CK, et al. Ionizing radiation absorption of vascular surgeons during endovascular procedures. J Vasc Surg 2007;46:455–9. [PubMed: 17826233]

19. Kalef-Ezra JA, Karavasilis S, Ziogas D, Dristiliaris D, Michalis LK, Matsagas M. Radiation burden of patients undergoing endovascular abdominal aortic aneurysm repair. J Vasc Surg 2009;49:283–7. [PubMed: 19216946]

20. Dijkstra ML, Eagleton MJ, Greenberg RK, Mastracci T, Hernandez A. Intraoperative C-arm cone-beam computed tomography in fenestrated/branched aortic endografting. J Vasc Surg 2011;53:583–90. [PubMed: 21129898]

21. Kobeiter H, Nahum J, Becquemin JP. Zero-contrast thoracic endovascular aortic repair using image fusion. Circulation 2011;124:e280–2. [PubMed: 21911788]

22. Kalef-Ezra JA, Karavasilis S, Kouvelos G, Dristiliaris D, Michalis LK, Matsagkas M. Endovascular abdominal aortic aneurysm repair: methods of radiological risk reduction. J Cardiovasc Surg Torino 2011;52:769–78.

23. Fossaceca R, Brambilla M, Guzzardi G, Cerini P, Renghi A, Valzano S, et al. The impact of radiological equipment on patient radiation exposure during endovascular aortic aneurysm repair. Eur Radiol 2012;22:2424–31. [PubMed: 22618524]

24. Maurel B, Martin-Gonzalez T, Chong D, Irwin A, Guimbretière G, Davis M, et al. A prospective observational trial of fusion imaging in infrarenal aneurysms. J Vasc Surg 2018;68:1706–13. [PubMed: 29804734]

25. Hertault A, Maurel B, Sobocinski J, Martin Gonzalez T, Le Roux M, Azzaoui R, et al. Impact of hybrid rooms with image fusion on radiation exposure during endovascular aortic repair. Eur J Vasc Endovasc Surg 2014;48:382–90. [PubMed: 25042331]

26. Tacher V, Lin M, Desgranges P, Deux JF, Grünhagen T, Becquemin JP, et al. Image guidance for endovascular repair of complex aortic aneurysms: comparison of two-dimensional and three-dimensional angiography and image fusion. J Vasc Interv Radiol 2013;24:1698–706. [PubMed: 24035418]

27. McNally MM, Scali ST, Feezor RJ, Neal D, Huber TS, Beck AW. Threedimensional fusion computed tomography decreases radiation exposure, procedure time, and contrast use during fenestrated endovascular aortic repair. J Vasc Surg 2015;61:309–16. [PubMed: 25175634]

28. Sailer AM, de Haan MW, Peppelenbosch AG, Jacobs MJ, Wildberger JE, Schurink GW. CTA with fluoroscopy image fusion guidance in endovascular complex aortic aneurysm repair. Eur J Vasc Endovasc Surg 2014;47:349–56. [PubMed: 24485850]

29. Hertault A, Maurel B, Midulla M, Bordier C, Desponds L, Saeed Kilani M, et al. Editor's choice – minimizing radiation exposure during endovascular procedures: basic knowledge, literature review, and reporting standards. Eur J Vasc Endovasc Surg 2015;50:21–36. [PubMed: 25818982]

30. Maurel B, Hertault A, Gonzalez TM, Sobocinski J, Le Roux M, Delaplace J, et al. Evaluation of visceral artery displacement by endograft delivery system insertion. J Endovasc Ther 2014;21:338–47.

31. Thibault B, Macle L, Mondésert B, Dubuc M, Shohoudi A, Dyrda K, et al. Reducing radiation exposure during procedures performed in the electrophysiology laboratory. J Cardiovasc Electrophysiol 2018;29: 308–15. [PubMed: 29064134]

32. Sanchez R, Vano E, Fernandez JM, Gallego JJ. Staff radiation doses in a real-time display inside the angiography room. Cardiovasc Interv Radiol 2010;33:1210–4.

33. Blaszak MA, Majewska N, Juszkat R, Majewski W. Dose-area product to patients during stent-graft treatment of thoracic and abdominal aortic aneurysms. Health Phys 2009;97:206–11. [PubMed: 19667803]

34. Doelare SAN, Smorenburg SPM, van Schaik TG, Blankensteijn JD, Wisselink W, Nederhoed JH, et al. Image fusion during standard and complex endovascular aortic repair, to fuse or not to fuse? A metaanalysis and additional data from a single-center retrospective cohort. J Endovasc Ther 2021;28:78–92. [PubMed: 32964768]

35. Goudeketting SR, Heinen SGH, Ünlü Ç, van den Heuvel DAF, de Vries JPM, van Strijen MJ, et al. Pros and cons of 3D image fusion in endovascular aortic repair: a systematic review and meta-analysis. J Endovasc Ther 2017;24:595–603. [PubMed: 28485198]

ARTICLE HIGHLIGHTS

- **Type of Research:** A single-center, retrospective cohort study

- **Key Findings:** In a study of 116 patients, augmented intelligence software, which incorporates a patient's preoperative computed tomography scan and live fluoroscopic images, resulted in a decreased radiation dose (1955 mGy vs 3755 mGy; $P = .004$), reduced fluoroscopy time (56 minutes vs 87 minutes; $P = .007$), and decreased contrast volume (123 mL vs 199 mL; $P < .0001$) in complex endovascular aortic repairs.

- **Take Home Message:** Surgical augmented intelligence can reduce the radiation dose, fluoroscopy time, and contrast volume in complex aortic repairs.
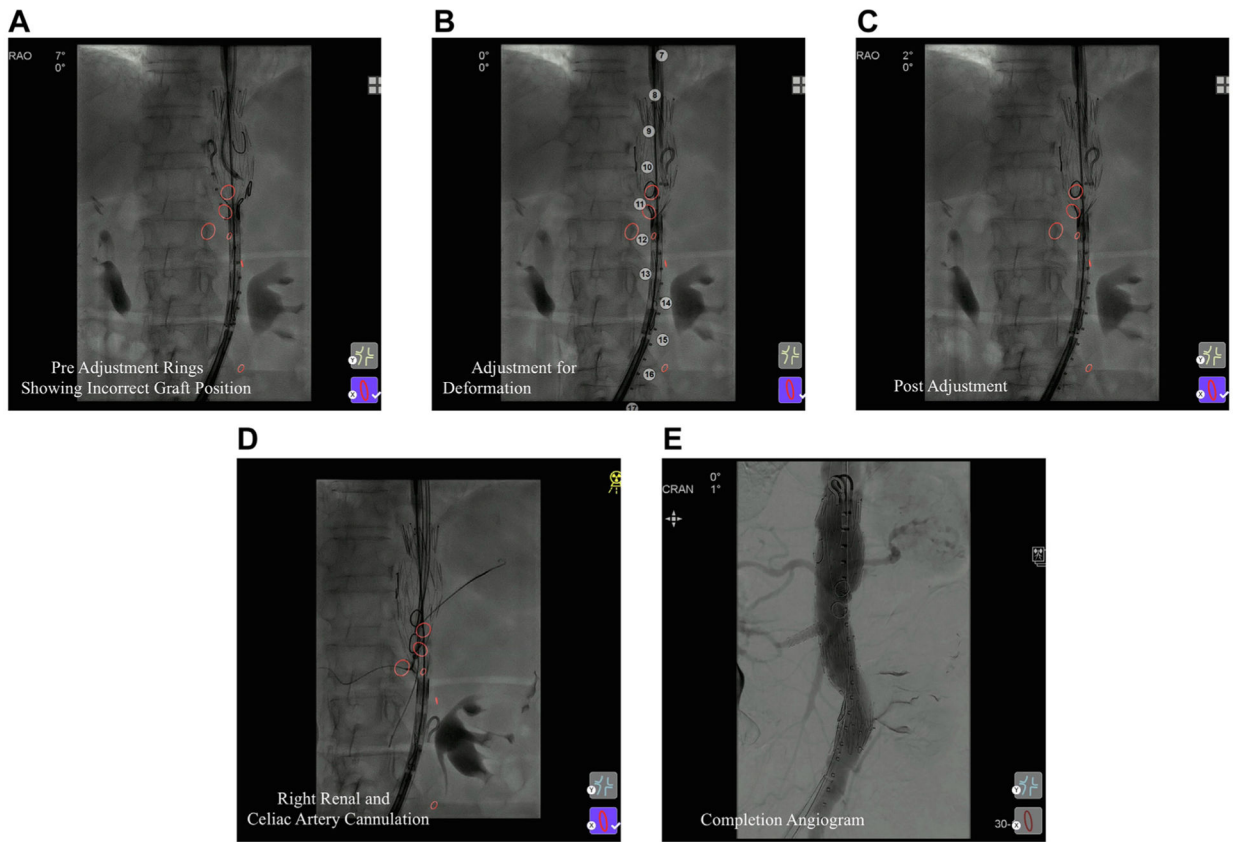
Fig.

Cydar EV map showing preadjustment rings showing incorrect graft position (**A**), adjustment for deformation (**B**), after adjustment (**C**), right renal and celiac artery cannulation (**D**), and completion angiogram (**E**).

Table I.

Baseline characteristics

Characteristic	WAI (n = 76; 65.5%)	WOAI (n = 40; 34.5%)	*P* value
Age, years	71.9 ± 12.0	75.5 ± 9.0	.075
BMI, kg/m^2	27.6 ± 5.4	26.1 ± 5.5	.166
Male sex	65 (85.5)	31 (77.5)	.277
Hispanic	12 (15.8)	3 (7.5)	.446
White race	45 (59.2)	28 (70.0)	.463
Chronic kidney disease	20 (26.3)	13 (32.5)	.101
Atrial fibrillation	17 (22.4)	7 (17.5)	.538
Congestive heart failure	13 (17.1)	4 (10.0)	.304
Peripheral arterial disease	15 (19.7)	7 (17.5)	.770
History of CABG or PCI	33 (43.4)	11 (27.5)	.093
Type 2 DM	12 (15.8)	5 (12.5)	.634
Coronary artery disease	36 (47.4)	17 (42.5)	.617
Hyperlipidemia	33 (43.4)	20 (50.0)	.499
Hypertension	65 (85.5)	33 (82.5)	.669
History of aneurysm other than aorta	6 (7.9)	2 (5.0)	.559
History of open aortic repair	3 (3.9)	2 (5.0)	.791
History of endovascular repair	26 (34.2)	15 (37.5)	.725
Family history of aortic aneurysm	1 (1.3)	4 (10.0)	.029
History of malignancy	17 (22.4)	10 (25.0)	.750
Aspirin use	44 (57.9)	23 (57.5)	.967
Clopidogrel use	13 (17.1)	6 (15.0)	.771
Statin use	55 (72.4)	26 (65.0)	.411
Anticoagulation use	22 (28.9)	6 (15.0)	.095

BMI, Body mass index; CABG, coronary artery bypass grafting; *DM*, diabetes mellitus; *PCI*, percutaneous coronary intervention; *WAI*, with augmented intelligence mapping; *WOAI*, without augmented intelligence mapping.

Data presented as mean ± standard deviation or number (%).

Table II.

Aneurysm characteristics

Characteristic	WAI (n = 76; 65.5%)	WOAI (n = 40; 34.5%)	P Value
Aneurysm size, mm	63.3 ± 17.9	66.2 ± 14.9	.351
Symptomatic	11 (14.5)	3 (7.5)	.273
Rupture	2 (2.6)	2 (5.0)	.506
Type of aneurysm			.380
Pararenal	27 (36.0)	17 (42.5)	
Juxtarenal	3 (4.0)	1 (2.5)	
Thoracoabdominal			
Type I	3 (4.0)	2 (5.0)	
Type II	9 (12.0)	1 (2.5)	
Type III	0	2 (5.0)	
Type IV	4 (5.3)	5 (12.5)	
Type V	6 (8.0)	2 (5.0)	
Type B dissection	5 (6.7)	1 (2.5)	
Thoracic	1 (1.3)	0 (0)	
Infrarenal[a]	13 (17.3)	6 (15.0)	
Other[b]	4 (5.3)	3 (7.5)	
Vessels treated, No.	2.6 ± 1.7	2.3 ± 1.5	.479

WAI, With augmented intelligence mapping; *WOAI*, without augmented intelligence mapping.

Data presented as mean ± standard deviation or number (%).

[a] Included endoleak and coil.

[b] Included visceral aneurysms and stenosis.

Table III.

Intraoperative outcomes (univariate analysis)

Outcome	WAI (n = 76; 65.5%)	WOAI (n = 40; 34.5%)	P value
Radiation exposure, mGy	1955 ± 1256	3755 ± 3638	.004
Fluoroscopy time, minutes	55.6 ± 39	86.9 ± 66	.008
Operative time, minutes	255 ± 109	284 ± 154	.294
Contrast volume, mL	122 ± 59	199 ± 97	<.0001
Estimated blood loss, mL	292.5 ± 423.7	232.3 ± 209.4	.308
Packed red blood cells transfused, U	0.4 ± 1.25	0.5 ± 1.04	.758
Intravenous fluid administered, mL	1523.7 ± 804.0	1816.3 ± 1047.4	.128
Spinal drain placement	11 (14.5)	9 (22.5)	.277
Arterial line placement	71 (93.4)	39 (97.5)	.346
Central line placement	20 (26.3)	8 (20.0)	.450
Radiation/BMI ratio	65.2 ± 46.7	139.7 ± 132.2	.001

BMI, Body mass index; *WAI*, with augmented intelligence mapping; *WOAI*, without augmented intelligence mapping.

Data presented as mean ± standard deviation or number (%).

Table IV.

Multivariate linear regression model[a]

Variable	Coefficient[b]	95% CI	P value	Adjusted R²
Operative time, minutes	−28.1	−74.0 to 17.9	.228	0.210
Contrast volume, mL	−77.3	−106.3 to −48.4	<.0001	0.275
Radiation exposure, mGy	−2002.1	−2822.2 to −1182.0	<.0001	0.397
Fluoroscopy time, minutes	−26.3	−45.2 to −7.4	.007	0.212
Estimated blood loss, mL	69.8	−76.7 to 216.4	.347	0.038
Packed red blood cells, U	0.01	−0.46 to 0.48	.971	0.037

CI, Confidence interval.

[a]Adjusted for age at surgery, sex, race, body mass index, smoking status, history of coronary artery disease, history of endovascular aortic repair, aneurysm size at presentation, and type of aneurysm; each model compared patients who had undergone surgery with augmented intelligence with patients who had undergone surgery without augmented intelligence.

[b]Reduction in covariate with use of fusion imaging.

Table V.

Thirty-day outcomes

Outcome	WAI (n = 76; 65.5%)	WOAI (n = 40; 34.5%)	P value
Length of stay	6.4 ± 7.9	6.9 ± 8.6	.752
Hematoma	4 (5.3)	0 (0)	.140
Pseudoaneurysm	3 (3.9)	0 (0)	.203
Pneumonia	3 (3.9)	3 (7.5)	.412
Urinary retention	1 (1.3)	1 (2.6)	.641
Urinary tract infection	3 (3.9)	3 (7.5)	.412
Stroke	3 (3.9)	0 (0)	.203
Renal failure	2 (2.6)	0 (0)	.301
Dialysis	3 (3.9)	0 (0)	.203
Bowel ischemia	1 (1.3)	0 (0)	.466
Lower extremity ischemia	1 (1.3)	0 (0)	.466
Paraplegia	2 (2.6)	1 (2.6)	.966
Death	4 (5.3)	0 (0)	.140

WAI, With augmented intelligence mapping; *WOAI*, without augmented intelligence mapping.

Data presented as mean ± standard deviation or number (%).